

1

A physiologically based pharmacokinetic model for CYP2E1 phenotyping via chlorzoxazone

Jonas Küttner^{1,*}, Jan Grzegorzewski¹, Hans-Michael Tautenhahn² and Matthias König^{1,*}

¹ Institute for Theoretical Biology, Institute of Biology, Humboldt University, Berlin, Germany

² Experimental Transplantation Surgery, Department of General, Visceral and Vascular Surgery, Jena University Hospital, Jena, Germany

Correspondence*:

Jonas Küttner
kuettnej@hu-berlin.de

Matthias König
koenigmx@hu-berlin.de

2 ABSTRACT

The cytochrome P450 (CYP) superfamily of enzymes plays a critical role in the metabolism of drugs, toxins, and endogenous and exogenous compounds. The activity of CYP enzymes can be influenced by a variety of factors, including genetics, diet, age, environmental factors, and disease. Among the major isoforms, CYP2E1 is of particular interest due to its involvement in the metabolism of various low molecular weight chemicals, including alcohols, pharmaceuticals, industrial solvents, and halogenated anesthetics. Metabolic phenotyping of CYPs based on the elimination of test compounds is a useful method for assessing in vivo activity, with chlorzoxazone being the primary probe drug for phenotyping of CYP2E1. The aim of this work was to investigate the effect of changes in CYP2E1 level and activity, ethanol consumption, ethanol abstinence, and liver impairment on the results of metabolic phenotyping with chlorzoxazone. To accomplish this, an extensive pharmacokinetic dataset for chlorzoxazone was established and a physiologically based pharmacokinetic (PBPK) model of chlorzoxazone and its metabolites, 6-hydroxychlorzoxazone and chlorzoxazone-O-glucuronide, was developed and validated. The model incorporates the effect of ethanol consumption on CYP2E1 levels and activity by extending the model with a core ethanol pharmacokinetic model and a CYP2E1 turnover model. The model accurately predicts pharmacokinetic data from several clinical studies and is able to estimate the effect of changes in CYP2E1 levels and activity on chlorzoxazone pharmacokinetics. Regular ethanol consumption induces CYP2E1 over two to three weeks, resulting in increased conversion of chlorzoxazone to 6-hydroxychlorzoxazone and a higher 6-hydroxychlorzoxazone/chlorzoxazone metabolic ratio. After ethanol withdrawal, CYP2E1 levels return to baseline within one week. Importantly, liver impairment has an opposite effect, resulting in reduced liver function via CYP2E1. In alcoholics with liver impairment who also consume ethanol, these factors will have opposite confounding effects on metabolic phenotyping with chlorzoxazone.

26 **Keywords:** PBPK, chlorzoxazone, CYP2E1, alcohol, ethanol

1 INTRODUCTION

Cytochrome P450 (CYP) enzymes are a superfamily of heme-containing enzymes that are critical for the oxidation of drugs, toxins, and both endogenous and exogenous compounds. CYP2E1 is a major isoform that contributes approximately 20-25% of the hepatic P450 protein pool and plays an important role in the metabolism of various low molecular weight chemicals, including alcohols, drugs, industrial solvents, and halogenated anesthetics (Couto et al., 2019; Raucy et al., 1993; Tanaka et al., 2000; Zhang et al., 2016).

To assess the in vivo activity of CYP enzymes, test substances that are specifically metabolized by these enzymes can be used as probe drugs. The pharmacokinetics of the test substance and its metabolites are used to determine the function of the enzyme. Chlorzoxazone has been established as the primary probe drug for metabolic phenotyping of CYP2E1 (Bachmann and Sarver, 1996; Dreisbach et al., 1995).

Chlorzoxazone is a muscle relaxant used to treat muscle spasms and low back pain (Liv, 2012). Its primary metabolism occurs in the liver via CYP2E1-mediated 6-hydroxylation. The resulting 6-hydroxychlorzoxazone is rapidly conjugated with glucuronic acid and excreted by the kidneys, with less than 2% of the administered dose recovered in the urine as free chlorzoxazone. No unconjugated 6-hydroxychlorzoxazone is detected in blood samples, indicating that chlorzoxazone is completely metabolized and the resulting 6-hydroxychlorzoxazone is conjugated within a single pass through the liver (Liv, 2012; de Vries et al., 1994; Desiraju et al., 1983).

Metabolic phenotyping of CYP2E1 using chlorzoxazone typically involves recording plasma concentrations of chlorzoxazone and its metabolites 6-hydroxychlorzoxazone and chlorzoxazone-O-glucuronide over a period of 8 hours. To measure both 6-hydroxychlorzoxazone and its glucuronide, a glucuronidase is often used to cleave the glucuronide group and measure the concentration of 6-hydroxychlorzoxazone and its glucuronide. Various pharmacokinetic parameters can be calculated from the metabolite time courses to assess the metabolic phenotype. Alternatively, the percentage of the chlorzoxazone dose recovered in urine as CZXOGlu has been used, which ranges from 39 to 74% and shows considerable interindividual variability (Desiraju et al., 1983; de Vries et al., 1994; Dreisbach et al., 1995; Frye et al., 1998; Girre et al., 1994; Lucas et al., 1993). The reason for this incomplete recovery is not clear and could be due to incomplete absorption or the presence of alternative metabolites. Simplified phenotyping methods based on the 6-hydroxychlorzoxazone/chlorzoxazone metabolic ratio after two or four hours from a single plasma sample have been established as a proxy for CYP2E1 metabolic activity.

Studies have shown that CYP1A1 and CYP1A2, in addition to CYP2E1, may contribute to the 6-hydroxylation of chlorzoxazone in human liver microsomes (Carriere et al., 1993; Ono et al., 1995; Yamamura et al., 2015), raising concerns about whether chlorzoxazone is a suitable phenotypic probe for measuring CYP2E1 activity. Cigarette smoking is known to induce CYP1A1 and CYP1A2 (Grzegorzewski et al., 2021a); however, two studies found no effect of tobacco smoking on chlorzoxazone metabolism in vivo (Girre et al., 1994; Lucas et al., 1999). In contrast, another study using a within-subject design reported an acceleration of chlorzoxazone metabolism (Benowitz et al., 2003). These results suggest that the contribution of CYP1A1 and CYP1A2 to chlorzoxazone metabolism is small and that 6-hydroxylation of chlorzoxazone is a good marker of CYP2E1 activity.

A thorough understanding of CYP2E1 regulation is important because it plays a critical role in activating prototoxins and can generate reactive oxygen species that can cause liver damage. Several factors, including genetics, diet, fasting, age, sex, environmental factors, and disease, can influence CYP2E1 activity. In particular, ethanol consumption has been shown to be a strong inducer of CYP2E1 metabolism. Several studies have shown that the liver microsomes of alcoholics have higher CYP2E1 protein levels compared

69 to non-drinkers or non-active drinkers (Mishin et al., 1998). In addition, numerous pharmacokinetic studies
70 have found that CYP2E1-mediated metabolism of chlorzoxazone is increased in alcoholics (Girre et al.,
71 1994; de la Maza et al., 2000; Mishin et al., 1998; Lucas et al., 1993).

72 The widespread consumption of ethanol worldwide makes it a particularly interesting inducer of CYP2E1.
73 While alcohol dehydrogenase is primarily responsible for ethanol metabolism in the liver, CYP2E1 can
74 also metabolize ethanol, albeit with a lower affinity (about 10 mM) than alcohol dehydrogenase (0.05-1
75 mM) (Jiang et al., 2020). Consequently, CYP2E1 plays a role in alcohol elimination at higher ethanol
76 concentrations, and its inducibility by ethanol contributes to metabolic tolerance in regular drinkers (Osna
77 et al., 2017). The regulation of CYP2E1 induction by ethanol is thought to involve transcriptional and
78 post-translational mechanisms. In human liver biopsy samples from recent drinkers, CYP2E1 mRNA levels
79 were found to be increased compared to non-drinkers, although the transcriptional regulation of CYP2E1
80 is not yet fully understood (Takahashi et al., 1993). In rats, several studies have shown that ethanol can
81 slow the degradation of CYP2E1 (Bardag-Gorce et al., 2002; Eliasson et al., 1988; Song et al., 1989).
82 Substrate binding can block the ubiquitination site of CYP2E1, making the enzyme inaccessible to the
83 ubiquitin-proteasome system (Banerjee et al., 2000; Roberts et al., 1995).

84 Chlorzoxazone-based metabolic phenotyping is widely used to evaluate alcoholic patients. However, a
85 critical question that remains unanswered is how social or abusive alcohol consumption and abstinence
86 from alcohol affect metabolic phenotyping via CYP2E1. Abusive alcohol use is associated with reduced
87 liver function and a spectrum of liver disease ranging from steatosis and nonalcoholic fatty liver disease
88 to alcoholic cirrhosis. The effect of liver disease and enzyme induction on metabolic phenotyping with
89 chlorzoxazone remains unclear.

90 The aim of this study was to use a physiologically based pharmacokinetic (PBPK) approach to investigate
91 the metabolic phenotyping of CYP2E1 using chlorzoxazone. Specifically, we aimed to address key
92 questions regarding how changes in CYP2E1 level and activity, ethanol consumption and abstinence, and
93 liver impairment might affect the results of metabolic phenotyping with chlorzoxazone.

2 MATERIAL AND METHODS

94 Data

95 A wide range of heterogeneous data was curated for model building (parameterization) and subsequent
96 model validation (comparison of model predictions with clinical data). We systematically searched PubMed
97 using the search string “(chlorzoxazone) AND (pharmacokinetics) AND ((CYP2E1) OR (P4502E1))”.
98 The result set of publications was searched for pharmacokinetic time course data and pharmacokinetic
99 parameters of chlorzoxazone. Studies reporting pharmacokinetic data in healthy and/or alcoholic subjects
100 were of particular interest. The initial corpus of publications was expanded based on references in the
101 initial set of publications. From the selected studies, information on the subjects and groups (e.g. age, sex,
102 disease, medication), the route of administration and dose of chlorzoxazone, and the pharmacokinetics of
103 chlorzoxazone were manually curated. Established data curation workflows for pharmacokinetic data were
104 applied to digitize data from figures, tables, and text (Grzegorzewski et al., 2021a). In addition data on the
105 pharmacokinetics of ethanol were curated from a single study identified by searching for “(ethanol) AND
106 (pharmacokinetics)” and manual screening of the results (Wilkinson et al., 1977). All data are available in
107 the pharmacokinetics database PK-DB (<https://pk-db.com>) (Grzegorzewski et al., 2021b). An overview of
108 the 29 studies with their respective chlorzoxazone and ethanol dosing protocols is provided in Tab. 1.

109 **Model**

110 The model was encoded in the Systems Biology Markup Language (SBML) (Hucka et al., 2019;
111 Keating et al., 2020) and developed using sbmlutils (König, 2021b), a collection of Python utilities
112 for building SBML models, and cy3sbml (König et al., 2012; König and Rodriguez, 2019), a visu-
113 alization software for SBML. The model is an ordinary differential equation (ODE) model which is
114 numerically solved by sbmlsim (König, 2021a) based on the high-performance SBML simulator libroad-
115 runner (Somogyi et al., 2015; Welsh et al., 2023). The model is available under the CC-BY 4.0 license at
116 <https://github.com/mattiaskoenig/chlorzoxazone-model>. Version 0.9.2 was used in this paper (Küttner and
117 König, 2023).

118 **PBPK model of chlorzoxazone and ethanol**

119 The physiologically based pharmacokinetic (PBPK) model is hierarchically organized (Fig. 1) and allows
120 simulation of the time courses of chlorzoxazone, 6-hydroxychlorzoxazone, chlorzoxazone-O-glucuronide,
121 and ethanol. The top layer represents the whole body and systemic circulation coupled with organ models
122 for lung, liver, kidney, intestine, and the rest compartment. Organs not relevant to chlorzoxazone metabolism
123 are included in the rest compartment. The metabolic and transport reactions for chlorzoxazone and its
124 metabolites are included in the organ models.

125 Transport reactions describe the import and export of chlorzoxazone, its metabolites, and ethanol between
126 plasma and organ compartments. Transport reactions are modeled by mass action kinetics of the form
127 $v = k_i \cdot (c_e - c_i \cdot f)$, where k_i is the import rate constant, f is a factor that scales the import rate to
128 achieve an equilibrium tissue distribution, and c_e and c_i are the plasma and compartment concentrations,
129 respectively.

130 All metabolic reactions of chlorzoxazone take place in the liver compartment. Chlorzoxazone is converted
131 to 6-hydroxychlorzoxazone (6-hydroxylation), 6-hydroxychlorzoxazone is converted to chlorzoxazone-
132 O-glucuronide (glucuronidation), and ethanol is eliminated. All metabolic reactions are modeled using
133 irreversible Michaelis-Menten kinetics of the form $v = v_{\max} \cdot \frac{S}{S+K_m}$.

134 **Ethanol induction of CYP2E1**

135 A protein stabilization model was implemented to describe the induction of CYP2E1 by ethanol. CYP2E1
136 was implemented as a dimensionless quantity (relative amount) that is produced and degraded at rates k_p
137 and k_d , respectively. The degradation rate of CYP2E1 was set based on the reported half-life of CYP2E1
138 t_{half} as $k_d^0 = \ln(2)/t_{\text{half}}$. A steady state concentration of 1 was obtained by assuming $k_p = k_d$.

139 The amount of CYP2E1 modulates the v_{\max} value of the 6-hydroxylation reaction catalyzed by CYP2E1.
140 Ethanol inhibits the degradation of CYP2E1, resulting in an increase in CYP2E1. The inhibition was
141 modeled by $k_{\text{deg}} = k_d^0/(1 + [\text{Eth}]/K_i)$ where k_d^0 is the degradation rate in the absence of alcohol, $[\text{Eth}]$ is
142 the ethanol concentration, and K_i is the inhibition constant of ethanol on the degradation.

143 **Model parametrization**

144 Values for organ volumes and tissue blood flows were taken from the literature (ICRP, 2002; Jones and
145 Rowland-Yeo, 2013). Eight model parameters were fitted for the chlorzoxazone metabolism model and four
146 parameters were fitted for the ethanol metabolism model. The parameters were determined by minimizing
147 the residuals between model predictions and time-course data.

148 A large subset of the curated clinical data was used to parameterize the chlorzoxazone model. This
149 data included time course data for plasma concentrations of chlorzoxazone, 6-hydroxychlorzoxazone, the
150 sum of 6-hydroxychlorzoxazone and chlorzoxazone-O-glucuronide, and urinary levels of chlorzoxazone-
151 O-glucuronide. It covered a wide range of chlorzoxazone doses from 0.005 mg to 750 mg and included
152 data for chlorzoxazone administration by tablet and oral solution. The data used to parameterize the
153 model were selected according to the following criteria Subjects were healthy and chlorzoxazone was
154 administered exclusively, i.e., no co-administration of other drugs or cocktail administrations. The ethanol
155 elimination model was parameterized using a single study that provided ethanol time course data for
156 four doses (Wilkinson et al., 1977). The optimization problem was solved using SciPy's least-squares
157 method and differential evolution algorithm (Virtanen et al., 2020). For the objective cost function F , which
158 depends on the parameters \vec{p} , a simple L2 norm consisting of the sum of weighted residuals was used.

$$F(\vec{p}) = 0.5 \cdot \sum_{i,k} (w_k \cdot w_{i,k} \cdot r_{i,k}(\vec{p}))^2 = \sum_{i,k} (w_k \cdot w_{i,k} \cdot (y_{i,k} - m_{i,k}(\vec{p})))^2 \quad (1)$$

159 where $r_{i,k} = (y_{i,k} - m_{i,k}(\vec{p}))$ is the residual of time point i in time course k for model prediction $m_{i,k}(\vec{p})$
160 and the corresponding data point $y_{i,k}$; $w_{i,k}$ is the weighting of the respective data point i in time course
161 k based on the error of the data point and w_k = the weighting factor of time course k . Weighting of time
162 courses was based on the number of subjects per study. The data used for the parameter fit is listed in Tab. 1.
163 The final parameter set given in Tab. 2 was determined using 10 runs of the local least squares optimization.

164 Pharmacokinetics parameters

165 Pharmacokinetic parameters of chlorzoxazone were calculated from the plasma-concentration time
166 courses and urinary excretion using standard non-compartmental methods (Urso et al., 2002). The elimination
167 rate k_{el} [1/min] was calculated via linear regression in logarithmic space in the decay phase. The area
168 under the curve AUC [mmole·min/L] was calculated via the trapezoidal rule and interpolated to infinity.
169 Clearance Cl [ml/min] was calculated as $Cl = k_{el} \cdot V_d$ with the apparent volume of distribution V_d as
170 $V_d = D / (AUC_\infty \cdot k_{el})$. D is the applied dose of chlorzoxazone.

3 RESULTS

171 3.1 Database of chlorzoxazone pharmacokinetics

172 To parameterize and validate the chlorzoxazone pharmacokinetic model, we curated a data set consisting
173 of 29 clinical trials. Most of the studies investigated drug-drug interactions, the effect of lifestyle and
174 physiological conditions such as alcoholism, obesity or diabetes, and the effect of different doses. In all
175 studies, chlorzoxazone was administered orally, mostly as a tablet and in rare cases as an oral solution.
176 The standard doses given were 250, 500 or 750 mg. In some cases, 400 mg was administered. In two
177 dose escalation studies, the doses ranged from 0.05 mg to 500 mg. In most studies, plasma concentrations
178 were measured for chlorzoxazone ($n=23$) and the metabolite 6-hydroxychlorzoxazone ($n=13$). The plasma
179 concentration of 6-hydroxychlorzoxazone was reported either as the concentration of unconjugated 6-
180 hydroxychlorzoxazone ($n=4$) or as the sum of unconjugated 6-hydroxychlorzoxazone and the glucuronide
181 chlorzoxazone-O-glucuronide ($n=9$). Some studies ($n=5$) also reported the time course of chlorzoxazone-
182 O-glucuronide recovered in urine, either as the amount or as the percentage of the administered dose
183 recovered.

184 **3.2 PBPK model of chlorzoxazone**

185 We developed a physiologically-based pharmacokinetics (PBPK) model for chlorzoxazone coupled with
186 a model of CYP2E1 regulation by ethanol (Fig. 1) using the curated data. The model is hierarchically
187 organized, with the top layer representing the whole body comprising the lung, liver, kidney, intestine,
188 and rest compartment, and transport via the systemic circulation. The intestine model (Fig. 1B) describes
189 the dissolution, absorption, and excretion of chlorzoxazone. Only a fraction of the administered chlor-
190 zoxazone dose is absorbed into the systemic circulation, with the remainder being excreted in the feces.
191 In the liver (Fig. 1C), chlorzoxazone is metabolized to 6-hydroxychlorzoxazone via CYP2E1 and subse-
192 quently converted to chlorzoxazone-O-glucuronide. The kidney model describes the renal excretion of
193 chlorzoxazone-O-glucuronide into the urine. Ethanol is absorbed into the systemic circulation (Fig. 1B) in
194 the intestine and eliminated in the liver (Fig. 1C). Ethanol affects chlorzoxazone metabolism by inhibiting
195 the degradation of CYP2E1 in the liver, resulting in increased CYP2E1 and conversion of chlorzoxazone.
196 The mathematical details of the model are described in the Materials and Methods.

197 **3.3 Model performance**

198 The model accurately predicts pharmacokinetic data from various clinical studies (Fig. 2). Our
199 model successfully described the concentration profiles of chlorzoxazone, 6-hydroxychlorzoxazone,
200 chlorzoxazone-O-glucuronide, and the amount of chlorzoxazone-O-glucuronide excreted in the urine
201 over time. The model was able to predict these profiles for doses ranging from 0.005 mg to 750 mg
202 administered as tablets or oral solutions in the studies we used for model parameterization (Bedada and
203 Neerati, 2016; Bedada and Boga, 2017; Bedada and Neerati, 2018; Burckart et al., 1998; de Vries et al.,
204 1994; Dreisbach et al., 1995; Frye et al., 1998; Girre et al., 1994; He et al., 2019; de la Maza et al., 2000;
205 Liangpunsakul et al., 2005; Lucas et al., 1993; Park et al., 2006; Rajnarayana et al., 2008; Vesell et al., 1995;
206 Wang et al., 2003; Hohmann et al., 2019; Witt et al., 2016). Refer to Tab. 1 for details on the respective
207 doses and application forms.

208 To investigate the dose-dependency of pharmacokinetic parameters, we analyzed the c_{max} of chlorzox-
209 azone and 6-hydroxychlorzoxazone, as well as the metabolic ratio at two hours for different doses per
210 body weight. Our model predicted an increase in both chlorzoxazone and 6-hydroxychlorzoxazone c_{max}
211 with increasing dose per body weight, and a decrease in the metabolic ratio at two hours. The predicted
212 dose-dependency was generally consistent with the observed pharmacokinetic data (Fig. 3).

213 **3.4 Effect of CYP2E1 on chlorzoxazone pharmacokinetics**

214 To explore the impact of changes in CYP2E1 activity and affinity on the conversion of chlorzoxazone
215 to 6-hydroxychlorzoxazone in metabolic phenotyping, we examined the effects of variations in v_{max}
216 and K_M by systematically scanning both parameters (Fig. 4). The time courses of chlorzoxazone and
217 its metabolites at a dose of 250 mg for v_{max} and K_M are shown in the left columns of Fig. 4A and
218 B, respectively. As CYP2E1 activity (v_{max}) increases above the reference value, chlorzoxazone plasma
219 concentrations decrease, while 6-hydroxychlorzoxazone, 6-hydroxychlorzoxazone + chlorzoxazone-O-
220 glucuronide and urinary recovery show minimal change. Conversely, decreasing CYP2E1 leads to increased
221 plasma concentrations of chlorzoxazone and reduced 6-hydroxychlorzoxazone, 6-hydroxychlorzoxazone +
222 chlorzoxazone-O-glucuronide during the first hours, followed by an increase after about 5 hours, with a
223 decrease in urinary recovery. The variation in CYP2E1 affinity (K_M) shows opposite effects.

224 The scan was performed for 250, 500, and 750 mg chlorzoxazone doses to evaluate the influence of
225 different chlorzoxazone doses. Pharmacokinetic parameters were calculated for each time course. The

226 2-hour metabolic rate (MR) and chlorzoxazone clearance increase with increasing CYP2E1 v_{max} , while the
227 AUC decreases. In contrast, the K_M of CYP2E1 shows an inverse relationship for these pharmacokinetic
228 parameters. The elimination rate k_{el} is not significantly affected by either v_{max} or K_M .

229 As expected, both changes in CYP2E1 activity (v_{max}) and affinity (K_M) have a significant impact on
230 chlorzoxazone pharmacokinetics and metabolic phenotyping results based on chlorzoxazone.

231 **3.5 CYP2E1 induction in alcoholic subjects**

232 Subsequently, we aimed to determine whether the observed changes in chlorzoxazone pharmacokinetics
233 and metabolic phenotyping results in alcoholics could be attributed to increased CYP2E1 activity resulting
234 from induction of CYP2E1 protein levels (Mishin et al., 1998). To determine whether our model could
235 qualitatively replicate the pharmacokinetic changes observed in alcoholic subjects, we compared a pa-
236 rameter scan for CYP2E1 activity with time course data from two clinical studies (Girre et al., 1994;
237 Lucas et al., 1993). Both studies contrasted a group of alcoholic subjects with a group of non-drinking
238 controls. A 500 mg dose of chlorzoxazone was administered, and plasma concentrations of chlorzoxazone,
239 6-hydroxychlorzoxazone, and chlorzoxazone-O-glucuronide, as well as urinary recovery, were measured
240 for at least 8 hours. The differences observed in both studies are consistent with the predictions of the
241 pharmacokinetic model (Fig. 5). In the alcoholic groups, the maximum concentrations achieved for chlor-
242 zoxazone are lower because elevated CYP2E1 levels accelerate chlorzoxazone hydroxylation. Despite the
243 significant differences in the chlorzoxazone curves, the maxima of the 6-hydroxychlorzoxazone curves
244 show only a modest increase. The urine recovery curves show similarities between the alcoholic and control
245 groups.

246 The 2-hour metabolic ratio (MR) is higher in alcoholics compared to controls. In conclusion, changes in
247 CYP2E1 activity resulting from the induction of CYP2E1 could account for the observed alterations in
248 chlorzoxazone pharmacokinetics in alcoholic patients.

249 **3.6 Changes in pharmacokinetic parameters due to changes in microsomal CYP2E1**

250 While numerous studies have indicated that in vitro CYP2E1 metabolism correlates with CYP2E1
251 quantity in human liver microsomes, only a handful of investigations have examined the relationship
252 between CYP2E1 amount and in vivo chlorzoxazone pharmacokinetics. To assess whether microsomal
253 protein quantity could serve as a proxy for CYP2E1 activity, we simulated two studies (Mishin et al., 1998;
254 Orellana et al., 2006) that reported the dependence of chlorzoxazone-O-glucuronide c_{max} and the 2-hour
255 MR on microsomal protein concentration, respectively. We normalized the reported protein concentration
256 to the mean of the abstinent group and the control for Mishin et al. (1998) and Orellana et al. (2006),
257 respectively.

258 In line with the data, c_{max} rises with increasing CYP2E1 activity. However, our model does not adequately
259 capture the overall increase of chlorzoxazone-O-glucuronide c_{max} reported by Mishin et al. (1998), as
260 it predicts saturated 6-hydroxychlorzoxazone and chlorzoxazone-O-glucuronide concentrations with an
261 induction of CYP2E1 activity (Fig. 6A). Conversely, the correlation between MR and microsomal protein
262 concentrations reported by Orellana et al. (2006) for the control, steatosis, and steatohepatitis groups was in
263 excellent agreement with the model (Fig. 6B).

264 **3.7 Effect of chronic ethanol consumption on the induction of CYP2E1 and CZX**
265 **pharmacokinetics**

266 Our model demonstrates that the accelerated metabolism of chlorzoxazone in induced subjects can be
267 attributed to an increase in CYP2E1 activity. Additionally, we explored the effects of chronic alcohol
268 consumption on CYP2E1 over time. To achieve this, we simulated a three-phase dosing protocol designed
269 to examine the impact of prolonged, moderate alcohol intake on CYP2E1 induction. In the first phase
270 (pre-drinking), lasting five days, no ethanol was administered. During the second phase (drinking), 40 g of
271 ethanol was administered daily at 8 pm for 30 days. In the final phase (withdrawal), no ethanol was provided
272 (Fig. 7). Throughout the simulation experiment, 500 mg of chlorzoxazone was administered every day at 8
273 am. We employed this model to predict data from clinical studies that investigated comparable experimental
274 protocols (Lucas et al., 1995; Mishin et al., 1998; Oneta et al., 2002). The previously described simulation
275 experiment was tailored to align with the protocols used in the respective studies, taking into account
276 factors such as dosage and physiological data of the subject groups, if available.

277 The conducted experimental studies either focused on the withdrawal phase (Lucas et al., 1995; Mishin
278 et al., 1998; Oneta et al., 2002) or the drinking phase (Oneta et al., 2002). For the withdrawal phase,
279 recently drinking alcoholics were tested with chlorzoxazone at multiple time points after their last drink.
280 Consequently, we initialized the corresponding simulation experiment with a CYP2E1 level that aligned
281 with the first measurement point reported in the clinical studies. We identified varying values for the initial
282 CYP2E1 amount, corresponding to a 3-fold, 2.7-fold, and a 1.575-fold CYP2E1 induction for Mishin1998,
283 Lucas1995, and Oneta2002, respectively. The initial CYP2E1 amount decayed exponentially over the
284 course of the experiment. By adjusting the CYP2E1 half-life to ensure the model output curve matched
285 the reported data, we determined a half-life of CYP2E1 induction of approximately 2 days (Fig. 7E,
286 G, H). Only one clinical study reported the dynamics of CYP2E1 induction in subjects who recently
287 began drinking(Oneta et al., 2002). We simulated this study using the drinking phase of the previously
288 described protocol and the CYP2E1 half-life determined from the withdrawal simulation experiments. The
289 model predicts an increase in the metabolic ratio that plateaus after 2 weeks (Fig. 7F). However, the data
290 from Oneta et al. (2002) show no saturation of induction after 4 weeks.

291 In summary, our model effectively predicts the changes in chlorzoxazone pharmacokinetics and metabolic
292 phenotyping due to alcohol induction and withdrawal, showing good agreement with the data.

293 **3.8 Compensatory effect of CYP2E1 induction and cirrhosis on metabolic phenotyping**

294 Chronic heavy drinking can lead to alcoholic liver disease, which can progress to alcoholic liver cirrhosis.
295 To assess the effects of cirrhosis in combination with CYP2E1 induction as observed in alcoholics on
296 liver function, we performed a parameter scan, scanning the CYP2E1 activity ($L1_f_cyp2e1$) over
297 a range from 0.5 to 4.0 and the cirrhosis parameter ($f_cirrhosis$) of our model for four cirrhosis
298 grades: control ($f_cirrhosis = 0$), mild cirrhosis ($f_cirrhosis=0.40$, CTP A), moderate cirrho-
299 sis ($f_cirrhosis=0.70$, CTP B), and severe cirrhosis ($f_cirrhosis=0.81$, CTP C) as previously
300 described (Köller et al., 2021a,b).

301 The cirrhosis parameter in our model determines the fraction by which the volume of the liver, as well
302 as the blood flow through the liver, is reduced. Because of this two-factor reduction in liver function,
303 the cirrhosis grade exhibits a non-linear effect on chlorzoxazone pharmacokinetics. To assess the actual
304 CYP2E1 activity in a cirrhotic liver, we calculated the effective CYP2E1 activity, which is determined

305 by ($f_{\text{eff}} = (1 - f_c^2 \cdot f_{\text{CYP}})$, where f_c is the cirrhosis grade, and f_{CYP} denotes the CYP2E1 activity. The
306 effective CYP2E1 activity directly translates to the predicted pharmacokinetic parameter (Fig. 8A).

307 To further study the counteracting effects of cirrhosis resulting in reduced liver function and increased
308 CYP2E1 activity, we scanned both parameters (Fig. 8B). Analysis of the isocline representing the simulated
309 MR for the reference values of both parameters ($f_{\text{cirrhosis}}=0$, $\text{LI_f_cyp2e1}=1$) reveals that a
310 2 to 3-fold induction of CYP2E1, typically seen in alcoholics, can compensate for mild liver cirrhosis
311 ($f_{\text{cirrhosis}}=0.4$) in the metabolic phenotyping result. Consequently, special care must be taken when
312 interpreting chlorzoxazone-based metabolic phenotyping results in patients with liver disease.

4 DISCUSSION

313 In this work we developed and validated a physiologically-based pharmacokinetics (PBPK) model for
314 chlorzoxazone used for CYP2E1 metabolic phenotyping. The model was developed and validated on a
315 large database of heterogeneous studies and is freely available in the open standard SBML (Keating et al.,
316 2020).

317 The model accurately predicted pharmacokinetic data from various studies. The model successfully
318 described the concentration profiles of chlorzoxazone and its metabolites for various doses. It demonstrated
319 that both changes in CYP2E1 activity and affinity significantly impacted chlorzoxazone pharmacokinetics
320 and metabolic phenotyping results. The model was then used to investigate the effects of alcohol on
321 CYP2E1 and chlorzoxazone pharmacokinetics, finding that changes in CYP2E1 activity due to alcohol
322 consumption could account for the observed alterations in chlorzoxazone pharmacokinetics in alcoholic
323 patients. Furthermore, the model effectively predicted changes in chlorzoxazone pharmacokinetics and
324 metabolic phenotyping due to alcohol induction and withdrawal. Lastly, the model was used to assess the
325 effects of cirrhosis in combination with CYP2E1 induction on liver function. The results indicated that
326 CYP2E1 induction in alcoholic patients with cirrhosis may serve as a compensatory mechanism, partially
327 maintaining metabolic capacity.

328 The pharmacokinetic data curated for this work displays considerable variability. Most of the studies
329 reported the kinetic data in the form of mean \pm SD or mean \pm SE. However, individual chlorzoxazone
330 time-courses show a large variability in c_{max} and t_{max} (de Vries et al., 1994). We fitted the model by
331 minimizing the distance between the time-course data and the model prediction, thus obtaining a parameter
332 set for an average patient. Fitting the model to individual time-courses may allow drawing conclusions
333 about the enzymatic equipment of individual subjects. Microsomal studies report immense interindividual
334 variability. We demonstrated that mapping the microsomal CYP2E1 concentration to the CYP2E1 activity
335 parameter of our model enables predicting the in vivo pharmacokinetics of subject groups (Fig. 6B). It
336 remains to be further investigated whether microsomal enzyme concentration distributions can be used to
337 predict the variability of CYP2E1 kinetics found in clinical pharmacokinetic studies.

338 We implemented an ethanol pharmacokinetic model capable of describing alcohol metabolism for various
339 doses of oral ethanol administration. Ethanol is primarily metabolized by alcohol dehydrogenase in the liver.
340 Through parameter fitting, we determined the K_M value of the enzymatic reaction to be 0.046 μM , which
341 corresponds to the reported k_M (0.05 μM) of the ADH1B*1 genotype of alcohol dehydrogenase (Jiang et al.,
342 2020). Although CYP2E1 is known to metabolize ethanol to acetaldehyde with a higher K_M than alcohol
343 dehydrogenase, playing a significant role at higher ethanol doses, we did not include this alternative route,
344 as the mono-enzymatic model adequately reproduced the experimental data.

345 We investigated whether a simple ethanol induction model for CYP2E1 could describe the acceleration
346 of chlorzoxazone metabolism in subjects who recently began drinking, as found by (Oneta et al., 2002).
347 We first determined the half-life of CYP2E1 by comparing our model output to data from several alcohol
348 withdrawal studies. With a first-order decay of CYP2E1 and a half-life of 1.8 d, the data was well-described.
349 However, the induction in subjects who recently started drinking followed more complex dynamics. With
350 the half-life we determined, our model reaches maximum induction after approximately two weeks, while
351 the data did not show saturation even after four weeks of drinking. Three individuals displayed a boost in
352 induction between the third and fourth weeks. This is the only study investigating the dynamics of CYP2E1
353 induction for individuals who started drinking, and the number of subjects (n=5) is too small to draw
354 definitive conclusions. Additionally, other metabolic state changes in the liver might occur with chronic
355 drinking.

356 Approximately 90% of drinkers who consume 4 to 5 drinks per day develop steatosis, the initial stage of
357 alcoholic liver disease. Prolonged alcohol consumption can lead to liver inflammation, fibrosis, cirrhosis,
358 and liver cancer (Osna et al., 2017). Depending on its severity, cirrhosis can cause reduced liver function
359 or even liver failure. Our model predicts that in individuals with mild to moderate cirrhotic livers, the
360 baseline level of metabolic function via CYP2E1 can be maintained due to CYP2E1 induction. However,
361 this is even more detrimental in cirrhotic livers, as the intact liver volume is reduced. Although the overall
362 metabolic activity is comparable to that of non-cirrhotic and non-induced livers, the CYP2E1 activity per
363 liver volume is increased. Since cirrhotic livers suffer from severe inflammation, the elevated CYP2E1
364 activity exposes the remaining tissue to greater oxidative stress, thereby accelerating the progression of the
365 disease.

366 In conclusion, we developed and validated a PBPK model for CYP2E1 phenotyping using chlorzoxazone.

CONFLICT OF INTEREST STATEMENT

367 The authors declare that the research was conducted in the absence of any commercial or financial
368 relationships that could be construed as a potential conflict of interest.

AUTHOR CONTRIBUTIONS

369 JK and MK conceived and designed the study, developed the computational model, curated the data,
370 implemented and performed the analysis, and drafted the manuscript. JG provided valuable support with
371 PK-DB, data curation, and modeling. All authors actively participated in the discussions of the results,
372 contributed to critical revisions of the manuscript, and approved the final version for submission.

FUNDING

373 MK was supported by the Federal Ministry of Education and Research (BMBF, Germany) within LiSyM by
374 grant number 031L0054 and ATLAS by grant number 031L0304B and by the German Research Foundation
375 (DFG) within the Research Unit Program FOR 5151 "QuaLiPerF (Quantifying Liver Perfusion-Function
376 Relationship in Complex Resection - A Systems Medicine Approach)" by grant number 436883643 and by
377 grant number 465194077 (Priority Programme SPP 2311, Subproject SimLivA). This work was supported
378 by the BMBF-funded de.NBI Cloud within the German Network for Bioinformatics Infrastructure (de.NBI)
379 (031A537B, 031A533A, 031A538A, 031A533B, 031A535A, 031A537C, 031A534A, 031A532B).

DATA AVAILABILITY STATEMENT

380 The datasets analyzed for this study can be found in PK-DB available from <https://pk-db.com>.

REFERENCES

- 381 (2012). *LiverTox: Clinical and Research Information on Drug-Induced Liver Injury* (Bethesda (MD)): 382 National Institute of Diabetes and Digestive and Kidney Diseases)
- 383 Bachmann, K. and Sarver, J. G. (1996). Chlorzoxazone as a single sample probe of hepatic CYP2E1 384 activity in humans. *Pharmacology* 52, 169–177. doi:10.1159/000139381
- 385 Banerjee, A., Kocarek, T. A., and Novak, R. F. (2000). Identification of a ubiquitination-Target/Substrate- 386 interaction domain of cytochrome P-450 (CYP) 2E1. *Drug Metabolism and Disposition: The Biological 387 Fate of Chemicals* 28, 118–124
- 388 Bardag-Gorce, F., Li, J., French, B. A., and French, S. W. (2002). Ethanol withdrawal induced CYP2E1 389 degradation in vivo, blocked by proteasomal inhibitor PS-341. *Free Radical Biology and Medicine* 32, 390 17–21. doi:10.1016/S0891-5849(01)00768-7
- 391 Bedada, S. K. and Boga, P. K. (2017). Effect of piperine on CYP2E1 enzyme activity of chlorzoxazone in 392 healthy volunteers. *Xenobiotica; the fate of foreign compounds in biological systems* 47, 1035–1041. 393 doi:10.1080/00498254.2016.1241450
- 394 Bedada, S. K. and Neerati, P. (2016). Resveratrol Pretreatment Affects CYP2E1 Activity of Chlorzoxazone 395 in Healthy Human Volunteers. *Phytotherapy research : PTR* 30, 463–468. doi:10.1002/ptr.5549
- 396 Bedada, S. K. and Neerati, P. (2018). The effect of quercetin on the pharmacokinetics of chlorzoxazone, 397 a CYP2E1 substrate, in healthy subjects. *European journal of clinical pharmacology* 74, 91–97. 398 doi:10.1007/s00228-017-2345-9
- 399 Benowitz, N. L., Peng, M., and Jacob, P., 3rd (2003). Effects of cigarette smoking and carbon monoxide 400 on chlorzoxazone and caffeine metabolism. *Clin. Pharmacol. Ther.* 74, 468–474. doi:10.1016/j.clpt. 401 2003.07.001
- 402 Burckart, G. J., Frye, R. F., Kelly, P., Branch, R. A., Jain, A., Fung, J. J., et al. (1998). Induction of 403 CYP2E1 activity in liver transplant patients as measured by chlorzoxazone 6-hydroxylation. *Clinical 404 pharmacology and therapeutics* 63, 296–302. doi:10.1016/S0009-9236(98)90161-8
- 405 Carriere, V., Goasduff, T., Ratanasavanh, D., Morel, F., Gautier, J. C., Guillouzo, A., et al. (1993). Both 406 cytochromes P450 2E1 and 1A1 are involved in the metabolism of chlorzoxazone. *Chemical Research 407 in Toxicology* 6, 852–857. doi:10.1021/tx00036a015
- 408 Chalasani, N., Gorski, J. C., Asghar, M. S., Asghar, A., Foresman, B., Hall, S. D., et al. (2003). Hepatic 409 cytochrome P450 2E1 activity in nondiabetic patients with nonalcoholic steatohepatitis. *Hepatology 410 (Baltimore, Md.)* 37, 544–550. doi:10.1053/jhep.2003.50095
- 411 Couto, N., Al-Majdoub, Z. M., Achour, B., Wright, P. C., Rostami-Hodjegan, A., and Barber, J. (2019). 412 Quantification of Proteins Involved in Drug Metabolism and Disposition in the Human Liver Using 413 Label-Free Global Proteomics. *Molecular Pharmaceutics* 16, 632–647. doi:10.1021/acs.molpharmaceut. 414 8b00941
- 415 de la Maza, M. P., Hirsch, S., Petermann, M., Suazo, M., Ugarte, G., and Bunout, D. (2000). Changes 416 in microsomal activity in alcoholism and obesity. *Alcoholism, clinical and experimental research* 24, 417 605–610. doi:10.1097/00000374-200005000-00004
- 418 de Simone, G., Devereux, R. B., Daniels, S. R., Mureddu, G., Roman, M. J., Kimball, T. R., et al. (1997). 419 Stroke volume and cardiac output in normotensive children and adults. Assessment of relations with 420 body size and impact of overweight. *Circulation* 95, 1837–1843. doi:10.1161/01.cir.95.7.1837

- 421 de Vries, J. D., Salphati, L., Horie, S., Becker, C. E., and Hoener, B. A. (1994). Variability in the disposition
422 of chlorzoxazone. *Biopharmaceutics & drug disposition* 15, 587–597. doi:10.1002/bdd.2510150706
- 423 Desiraju, R. K., Renzi, N. L., Nayak, R. K., and Ng, K.-T. (1983). Pharmacokinetics of Chlorzoxazone in
424 Humans. *Journal of Pharmaceutical Sciences* 72, 991–994. doi:10.1002/jps.2600720905
- 425 Dreisbach, A. W., Ferencz, N., Hopkins, N. E., Fuentes, M. G., Rege, A. B., George, W. J., et al. (1995).
426 Urinary excretion of 6-hydroxychlorzoxazone as an index of CYP2E1 activity. *Clinical pharmacology*
427 and *therapeutics* 58, 498–505. doi:10.1016/0009-9236(95)90169-8
- 428 Eap, C. B., Schnyder, C., Besson, J., Savary, L., and Buclin, T. (1998). Inhibition of CYP2E1 by
429 chlormethiazole as measured by chlorzoxazone pharmacokinetics in patients with alcoholism and in
430 healthy volunteers. *Clinical pharmacology and therapeutics* 64, 52–57. doi:10.1016/S0009-9236(98)
431 90022-4
- 432 Eliasson, E., Johansson, I., and Ingelman-Sundberg, M. (1988). Ligand-dependent maintenance of ethanol-
433 inducible cytochrome P-450 in primary rat hepatocyte cell cultures. *Biochemical and Biophysical*
434 *Research Communications* 150, 436–443. doi:10.1016/0006-291X(88)90539-6
- 435 Ernstgard, L., Warholm, M., and Johanson, G. (2004). Robustness of chlorzoxazone as an in vivo
436 measure of cytochrome P450 2E1 activity. *British Journal of Clinical Pharmacology* 58, 190–200.
437 doi:10.1111/j.1365-2125.2004.02132.x
- 438 Frye, R. F., Adedoyin, A., Mauro, K., Matzke, G. R., and Branch, R. A. (1998). Use of chlorzoxazone
439 as an in vivo probe of cytochrome P450 2E1: Choice of dose and phenotypic trait measure. *Journal of*
440 *clinical pharmacology* 38, 82–89. doi:10.1002/j.1552-4604.1998.tb04381.x
- 441 Girre, C., Lucas, D., Hispard, E., Menez, C., Dally, S., and Menez, J. F. (1994). Assessment of cytochrome
442 P4502E1 induction in alcoholic patients by chlorzoxazone pharmacokinetics. *Biochemical pharmacology*
443 47, 1503–1508. doi:10.1016/0006-2952(94)90524-x
- 444 Grzegorzewski, J., Bartsch, F., Köller, A., and König, M. (2021a). Pharmacokinetics of Caffeine: A
445 Systematic Analysis of Reported Data for Application in Metabolic Phenotyping and Liver Function
446 Testing. *Frontiers in Pharmacology* 12, 752826. doi:10.3389/fphar.2021.752826
- 447 Grzegorzewski, J., Brandhorst, J., Green, K., Eleftheriadou, D., Duport, Y., Barthorscht, F., et al. (2021b).
448 PK-DB: Pharmacokinetics database for individualized and stratified computational modeling. *Nucleic*
449 *Acids Research* 49, D1358–D1364. doi:10.1093/nar/gkaa990
- 450 He, J., Li, N., Xu, J., Zhu, J., Yu, Y., Chen, X., et al. (2019). An LC-MS/MS Validated Method for
451 Quantification of Chlorzoxazone in Human Plasma and Its Application to a Bioequivalence Study.
452 *Journal of chromatographic science* 57, 751–757. doi:10.1093/chromsci/bmz052
- 453 Herman, I. P. (2016). *Physics of the Human Body* (Springer)
- 454 Hohmann, N., Blank, A., Burhenne, J., Suzuki, Y., Mikus, G., and Haefeli, W. E. (2019). Simultaneous
455 phenotyping of CYP2E1 and CYP3A using oral chlorzoxazone and midazolam microdoses. *British*
456 *journal of clinical pharmacology* 85, 2310–2320. doi:10.1111/bcp.14040
- 457 Hucka, M., Bergmann, F. T., Chaouiya, C., Dräger, A., Hoops, S., Keating, S. M., et al. (2019). The
458 Systems Biology Markup Language (SBML): Language Specification for Level 3 Version 2 Core Release
459 2. *Journal of Integrative Bioinformatics* 16. doi:10.1515/jib-2019-0021
- 460 Hukkanen, J., Jacob III, P., Peng, M., Dempsey, D., and Benowitz, N. L. (2010). Effects of nicotine
461 on cytochrome P450 2A6 and 2E1 activities. *British journal of clinical pharmacology* 69, 152–159.
462 doi:10.1111/j.1365-2125.2009.03568.x
- 463 ICRP (2002). Basic anatomical and physiological data for use in radiological protection: reference values.
464 a report of age- and gender-related differences in the anatomical and physiological characteristics of
465 reference individuals. icrp publication 89. *Annals of the ICRP* 32, 5–265

- 466 Jiang, Y., Zhang, T., Kusumanchi, P., Han, S., Yang, Z., and Liangpunsakul, S. (2020). Alcohol
467 Metabolizing Enzymes, Microsomal Ethanol Oxidizing System, Cytochrome P450 2E1, Catalase, and
468 Aldehyde Dehydrogenase in Alcohol-Associated Liver Disease. *Biomedicines* 8, 50. doi:10.3390/
469 biomedicines8030050
- 470 Jones, H. and Rowland-Yeo, K. (2013). Basic concepts in physiologically based pharmacokinetic modeling
471 in drug discovery and development. *CPT: pharmacometrics & systems pharmacology* 2, e63. doi:10.
472 1038/psp.2013.41
- 473 Keating, S. M., Waltemath, D., König, M., Zhang, F., Dräger, A., Chaouiya, C., et al. (2020). SBML Level
474 3: An extensible format for the exchange and reuse of biological models. *Molecular Systems Biology* 16.
475 doi:10.15252/msb.20199110
- 476 Kharasch, E. D., Thummel, K. E., Mhyre, J., and Lillibridge, J. H. (1993). Single-dose disulfiram inhibition
477 of chlorzoxazone metabolism: A clinical probe for P450 2E1. *Clinical pharmacology and therapeutics*
478 53, 643–650. doi:10.1038/clpt.1993.85
- 479 Köller, A., Grzegorzewski, J., and König, M. (2021a). Physiologically based modeling of the effect of
480 physiological and anthropometric variability on indocyanine green based liver function tests. *Frontiers
481 in physiology* , 2043
- 482 Köller, A., Grzegorzewski, J., Tautenhahn, H.-M., and König, M. (2021b). Prediction of survival after
483 partial hepatectomy using a physiologically based pharmacokinetic model of indocyanine green liver
484 function tests. *Frontiers in physiology* , 1975
- 485 [Dataset] König, M. (2021a). Sbmlsim: SBML simulation made easy. Zenodo. doi:10.5281/ZENODO.
486 5531088
- 487 [Dataset] König, M. (2021b). Sbmlutils: Python utilities for SBML. Zenodo. doi:10.5281/ZENODO.
488 5546603
- 489 König, M., Dräger, A., and Holzhütter, H.-G. (2012). CySBML: A Cytoscape plugin for SBML.
490 *Bioinformatics* 28, 2402–2403. doi:10.1093/bioinformatics/bts432
- 491 [Dataset] König, M. and Rodriguez, N. (2019). Matthiaskoenig/cy3sbml: Cy3sbml-v0.3.0 - SBML for
492 Cytoscape. Zenodo. doi:10.5281/ZENODO.3451319
- 493 [Dataset] Küttner, J. and König, M. (2023). Physiologically based pharmacokinetic (PBPK) model of
494 chlorzoxazone. Zenodo. doi:10.5281/ZENODO.7821956
- 495 Liangpunsakul, S., Kolwankar, D., Pinto, A., Gorski, J. C., Hall, S. D., and Chalasani, N. (2005). Activity
496 of CYP2E1 and CYP3A enzymes in adults with moderate alcohol consumption: A comparison with
497 nonalcoholics. *Hepatology (Baltimore, Md.)* 41, 1144–1150. doi:10.1002/hep.20673
- 498 Lucas, D., Berthou, F., Girre, C., Poitrenaud, F., and Ménez, J.-F. (1993). High-performance liquid chro-
499 matographic determination of chlorzoxazone and 6-hydroxychlorzoxazone in serum: A tool for indirect
500 evaluation of cytochrome P4502E1 activity in humans. *Journal of Chromatography B: Biomedical
501 Sciences and Applications* 622, 79–86. doi:10.1016/0378-4347(93)80252-Y
- 502 Lucas, D., Ferrara, R., Gonzalez, E., Bodenez, P., Albores, A., Manno, M., et al. (1999). Chlorzoxazone,
503 a selective probe for phenotyping CYP2E1 in humans. *Pharmacogenetics* 9, 377–388. doi:10.1097/
504 00008571-199906000-00013
- 505 Lucas, D., Ménez, C., Girre, C., Bodénez, P., Hispard, E., and Ménez, J. F. (1995). Decrease in cytochrome
506 P4502E1 as assessed by the rate of chlorzoxazone hydroxylation in alcoholics during the withdrawal
507 phase. *Alcoholism, clinical and experimental research* 19, 362–366. doi:10.1111/j.1530-0277.1995.
508 tb01516.x

- 509 Mishin, V. M., Rosman, A. S., Basu, P., Kessova, I., Oneta, C. M., and Lieber, C. S. (1998). Chlorzoxazone
510 pharmacokinetics as a marker of hepatic cytochrome P4502E1 in humans. *The American Journal of
511 Gastroenterology* 93, 2154–2161. doi:10.1111/j.1572-0241.1998.00612.x
- 512 Oneta, C. M., Lieber, C. S., Li, J., Rüttimann, S., Schmid, B., Lattmann, J., et al. (2002). Dynamics of
513 cytochrome P4502E1 activity in man: Induction by ethanol and disappearance during withdrawal phase.
514 *Journal of hepatology* 36, 47–52. doi:10.1016/s0168-8278(01)00223-9
- 515 Ono, S., Hatanaka, T., Hotta, H., Tsutsui, M., Satoh, T., and Gonzalez, F. J. (1995). Chlorzoxazone
516 is metabolized by human CYP1A2 as well as by human CYP2E1. *Pharmacogenetics* 5, 143–150.
517 doi:10.1097/00008571-199506000-00002
- 518 Orellana, M., Rodrigo, R., Varela, N., Araya, J., Poniachik, J., Csendes, A., et al. (2006). Relationship
519 between in vivo chlorzoxazone hydroxylation, hepatic cytochrome P450 2E1 content and liver injury in
520 obese non-alcoholic fatty liver disease patients. *Hepatology Research* 34, 57–63. doi:10.1016/j.hepres.
521 2005.10.001
- 522 O’Shea, D., Davis, S. N., Kim, R. B., and Wilkinson, G. R. (1994). Effect of fasting and obesity in humans
523 on the 6-hydroxylation of chlorzoxazone: A putative probe of CYP2E1 activity. *Clinical pharmacology
524 and therapeutics* 56, 359–367. doi:10.1038/clpt.1994.150
- 525 Osna, N. A., Donohue, T. M., and Kharbanda, K. K. (2017). Alcoholic Liver Disease: Pathogenesis and
526 Current Management. *Alcohol Research: Current Reviews* 38, 147–161
- 527 Park, J.-Y., Kim, K.-A., Park, P.-W., and Ha, J.-M. (2006). Effect of high-dose aspirin on CYP2E1 activity
528 in healthy subjects measured using chlorzoxazone as a probe. *Journal of clinical pharmacology* 46,
529 109–114. doi:10.1177/0091270005282635
- 530 Rajnarayana, K., Venkatesham, A., Nagulu, M., Srinivas, M., and Krishna, D. R. (2008). Influence of
531 diosmin pretreatment on the pharmacokinetics of chlorzoxazone in healthy male volunteers. *Drug
532 metabolism and drug interactions* 23, 311–321. doi:10.1515/dmdi.2008.23.3-4.311
- 533 Raucy, J. L., Kraner, J. C., and Lasker, J. M. (1993). Bioactivation of Halogenated Hydrocarbons by
534 Cytochrome P4502E1. *Critical Reviews in Toxicology* 23, 1–20. doi:10.3109/10408449309104072
- 535 Roberts, B. J., Song, B.-J., Soh, Y., Park, S. S., and Shoaf, S. E. (1995). Ethanol Induces CYP2E1 by Protein
536 Stabilization. *Journal of Biological Chemistry* 270, 29632–29635. doi:10.1074/jbc.270.50.29632
- 537 Somogyi, E. T., Bouteiller, J.-M., Glazier, J. A., König, M., Medley, J. K., Swat, M. H., et al. (2015).
538 libRoadRunner: A high performance SBML simulation and analysis library. *Bioinformatics* 31, 3315–
539 3321. doi:10.1093/bioinformatics/btv363
- 540 Song, B. J., Veech, R. L., Park, S. S., Gelboin, H. V., and Gonzalez, F. J. (1989). Induction of Rat Hepatic
541 N-Nitrosodimethylamine Demethylase by Acetone Is Due to Protein Stabilization. *Journal of Biological
542 Chemistry* 264, 3568–3572. doi:10.1016/S0021-9258(18)94103-7
- 543 Takahashi, T., Lasker, J. M., Rosman, A. S., and Lieber, C. S. (1993). Induction of cytochrome P-4502E1
544 in the human liver by ethanol is caused by a corresponding increase in encoding messenger RNA.
545 *Hepatology* 17, 236–245. doi:10.1002/hep.1840170213
- 546 Tanaka, E., Terada, M., and Misawa, S. (2000). Cytochrome P450 2E1: Its clinical and toxicological role.
547 *Journal of Clinical Pharmacy and Therapeutics* 25, 165–175. doi:10.1046/j.1365-2710.2000.00282.x
- 548 Urso, R., Blardi, P., and Giorgi, G. (2002). A short introduction to pharmacokinetics. *European review for
549 medical and pharmacological sciences* 6, 33–44
- 550 Vander, J. S., A. (2001). Human physiology: The mechanisms of body function. *McGraw-Hill higher
551 education*

- 552 Vesell, E. S., Seaton, T. D., and A-Rahim, Y. I. (1995). Studies on interindividual variations of
553 CYP2E1 using chlorzoxazone as an in vivo probe. *Pharmacogenetics* 5, 53–57. doi:10.1097/
554 00008571-199502000-00007
- 555 Virtanen, P., Gommers, R., Oliphant, T. E., Haberland, M., Reddy, T., Cournapeau, D., et al. (2020).
556 SciPy 1.0: Fundamental Algorithms for Scientific Computing in Python. *Nature Methods* 17, 261–272.
557 doi:10.1038/s41592-019-0686-2
- 558 Wang, Z., Hall, S. D., Maya, J. F., Li, L., Asghar, A., and Gorski, J. C. (2003). Diabetes mellitus increases
559 the in vivo activity of cytochrome P450 2E1 in humans. *British journal of clinical pharmacology* 55,
560 77–85. doi:10.1046/j.1365-2125.2003.01731.x
- 561 Welsh, C., Xu, J., Smith, L., König, M., Choi, K., and Sauro, H. M. (2023). libRoadRunner 2.0: A
562 high performance SBML simulation and analysis library. *Bioinformatics* 39, btac770. doi:10.1093/
563 bioinformatics/btac770
- 564 Wilkinson, P. K., Sedman, A. J., Sakmar, E., Kay, D. R., and Wagner, J. G. (1977). Pharmacokinetics of
565 ethanol after oral administration in the fasting state. *Journal of Pharmacokinetics and Biopharmaceutics*
566 5, 207–224. doi:10.1007/BF01065396
- 567 Witt, L., Suzuki, Y., Hohmann, N., Mikus, G., Haefeli, W. E., and Burhenne, J. (2016). Ultrasensitive
568 quantification of the CYP2E1 probe chlorzoxazone and its main metabolite 6-hydroxychlorzoxazone in
569 human plasma using ultra performance liquid chromatography coupled to tandem mass spectrometry after
570 chlorzoxazone microdosing. *Journal of chromatography. B, Analytical technologies in the biomedical
571 and life sciences* 1027, 207–213. doi:10.1016/j.jchromb.2016.05.049
- 572 Yamamura, Y., Koyama, N., and Umehara, K. (2015). Comprehensive kinetic analysis and influence of
573 reaction components for chlorzoxazone 6-hydroxylation in human liver microsomes with CYP antibodies.
574 *Xenobiotica; the fate of foreign compounds in biological systems* 45, 353–360. doi:10.3109/00498254.
575 2014.985760
- 576 Zhang, H.-F., Wang, H.-H., Gao, N., Wei, J.-Y., Tian, X., Zhao, Y., et al. (2016). Physiological Content and
577 Intrinsic Activities of 10 Cytochrome P450 Isoforms in Human Normal Liver Microsomes. *The Journal
578 of Pharmacology and Experimental Therapeutics* 358, 83–93. doi:10.1124/jpet.116.233635

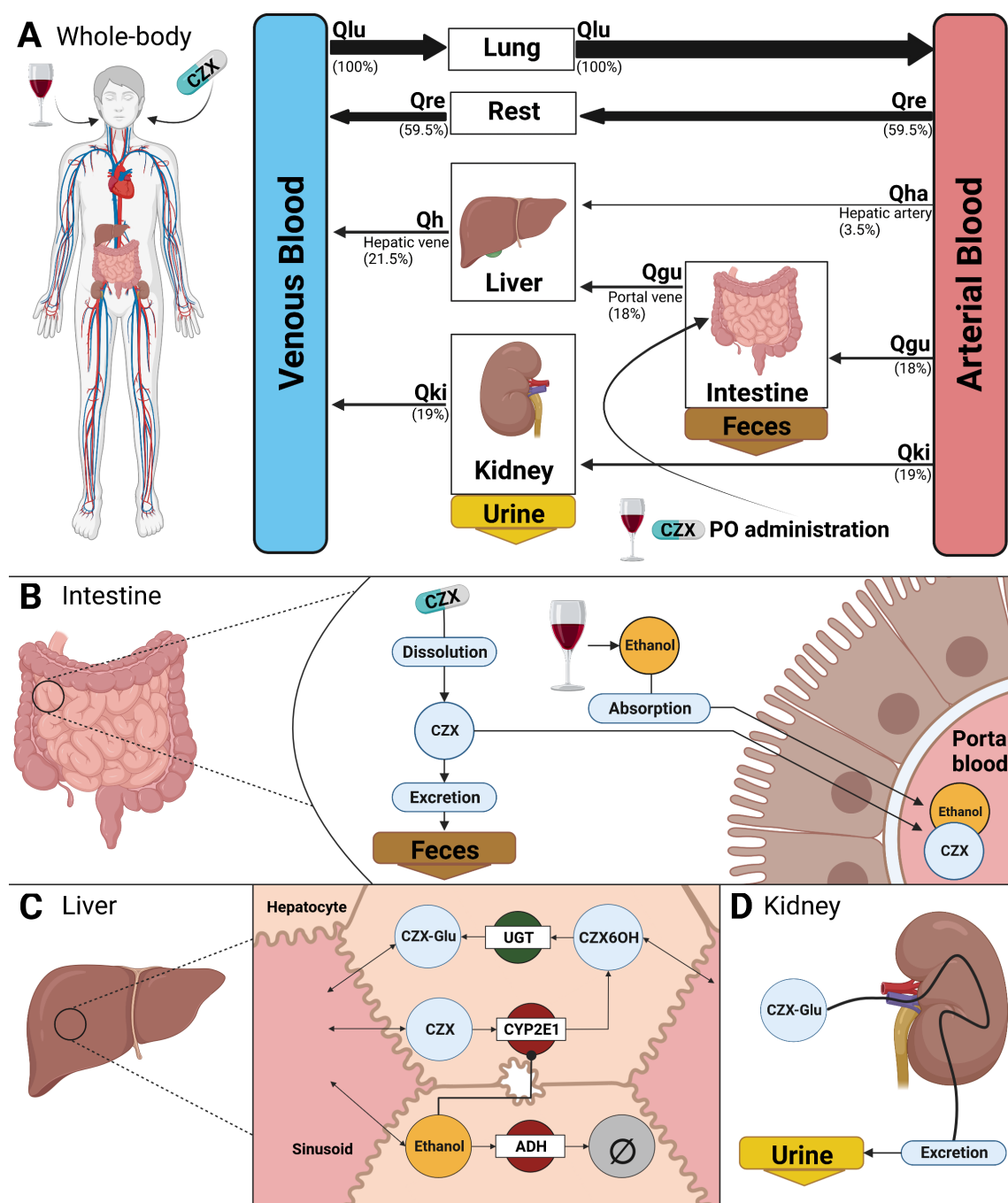


Figure 1: Human PKPK model of chlorzoxazone and ethanol. (A) Whole body model consisting of liver, kidney, lung and rest compartment. Organs with minor relevance for chlorzoxazone are not modelled explicitly and are condensed in the rest compartment. The organs are connected *via* the systemic circulation, denoted by arrows. The arrow widths are proportional to the relative blood flow through the corresponding route. chlorzoxazone and ethanol are administered orally. (B) Intestine model consisting of dissolution, absorption and excretion for chlorzoxazone. The dissolution depends on the application form (tablet, oral solution) and determines how fast chlorzoxazone becomes available for absorption. Only a fraction of the dose is absorbed into the systemic circulation, with the remainder being excreted into the feces. Administered ethanol is instantly available for absorption and fully absorbed. (C) Liver model for the conversion chlorzoxazone and the elimination of ethanol. chlorzoxazone is converted to 6-hydroxychlorzoxazone mediated by CYP2E1. 6-hydroxychlorzoxazone is glucuronidated by UGT. Ethanol is eliminated by the alcohol dehydrogenase. Ethanol metabolism by CYP2E1 is neglected. CYP2E1 is induced by the presences of ethanol. (D) Kidney model of urinary excretion of chlorzoxazone-O-glucuronide. Created with BioRender.com

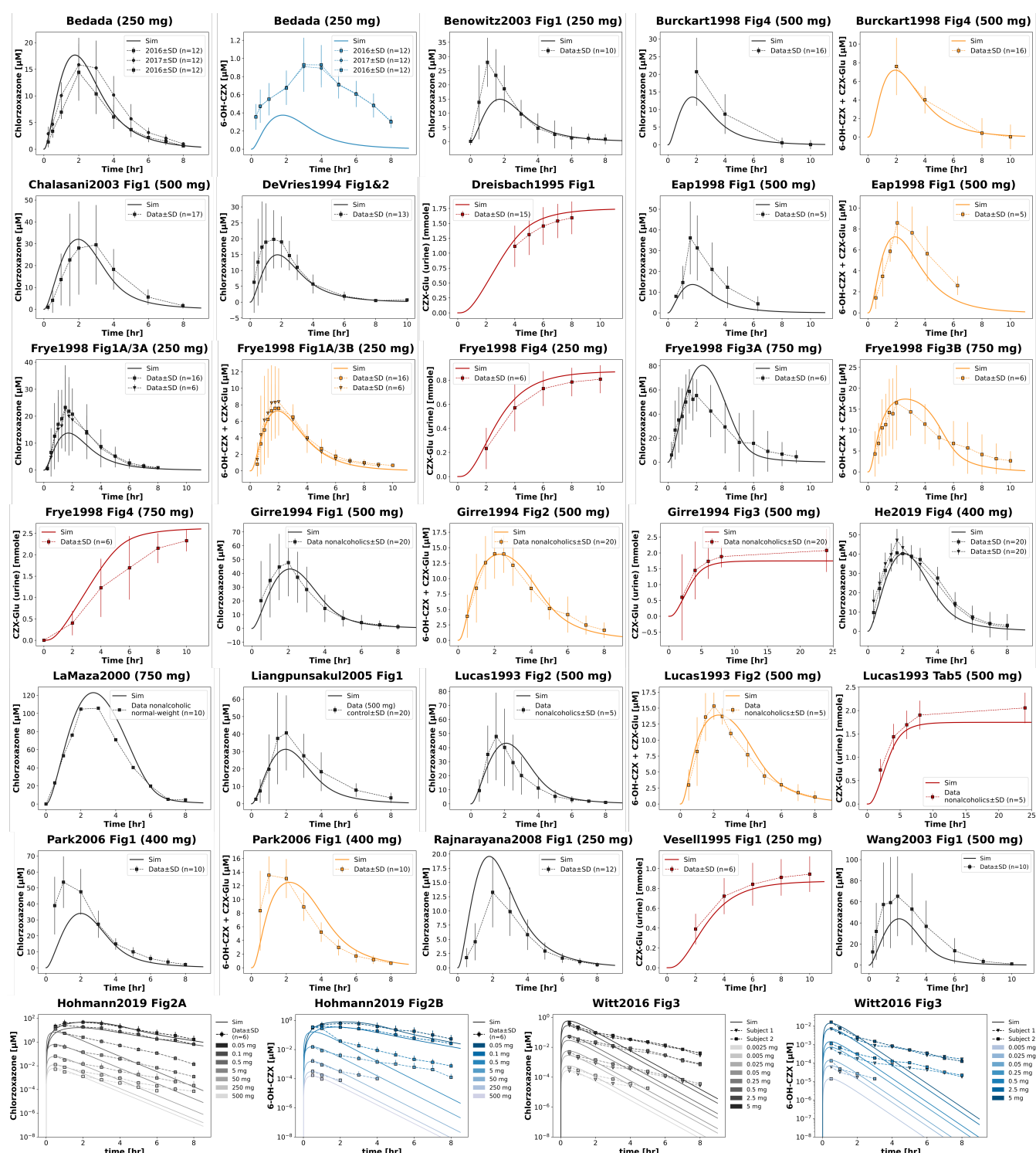


Figure 2: Performance of the chlorzoxazone model The model simulates time courses for the plasma concentrations of chlorzoxazone, chlorzoxazone-O-glucuronide, 6-hydroxychlorzoxazone and the urinary amounts of chlorzoxazone-O-glucuronide. The time-courses shown in this plot were used for parameter fitting, except for the 6-hydroxychlorzoxazone time-courses from the Bedada studies. Studies were selected when they met the following criteria: (1) only chlorzoxazone was administered (no cocktail or co-administrations) (2) the subjects are adults (3) data for more than one subject was reported. Data from (Bedada and Neerati, 2016; Bedada and Boga, 2017; Bedada and Neerati, 2018; Benowitz et al., 2003; Burckart et al., 1998; Chalasani et al., 2003; Dreisbach et al., 1995; Eap et al., 1998; Girre et al., 1994; He et al., 2019; de la Maza et al., 2000; Liangpunsakul et al., 2005; Lucas et al., 1993; Park et al., 2006; Rajnarayana et al., 2008; Vesell et al., 1995; Wang et al., 2003; Hohmann et al., 2019; Witt et al., 2016).

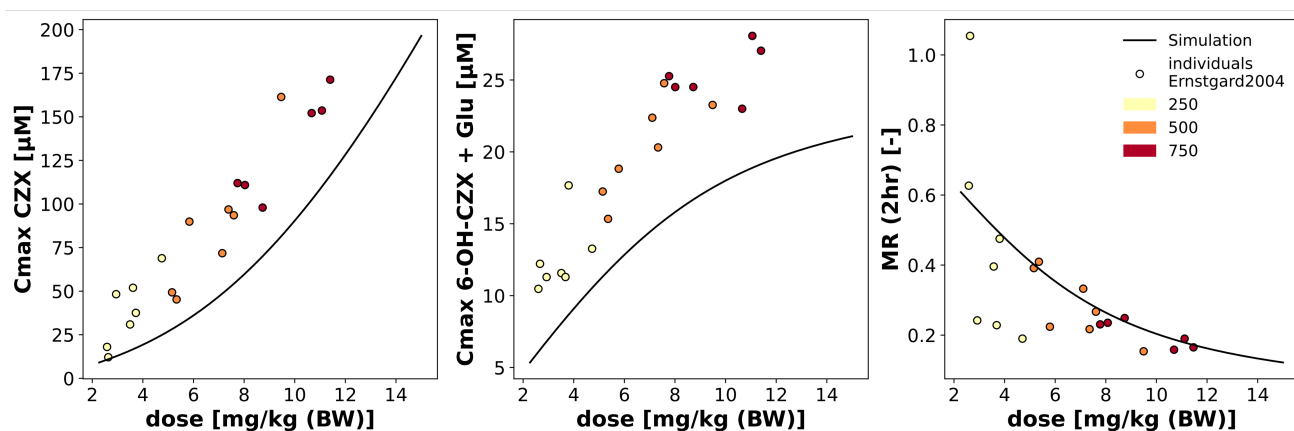


Figure 3: Prediction of pharmacokinetics based on body weight normalized dose. The model body weight was scanned linearly from 50 to 110 kg for a doses of 250, 500, and 750 mg. For each time-course, cmax of chlorzoxazone, 6-hydroxychlorzoxazone + chlorzoxazone-O-glucuronide, and the metabolic ratio at 2hr, were calculated. The results were sorted by the dose normalized by body weight (black solid lines). The simulation was compared to individual data from (Ernstgard et al., 2004)

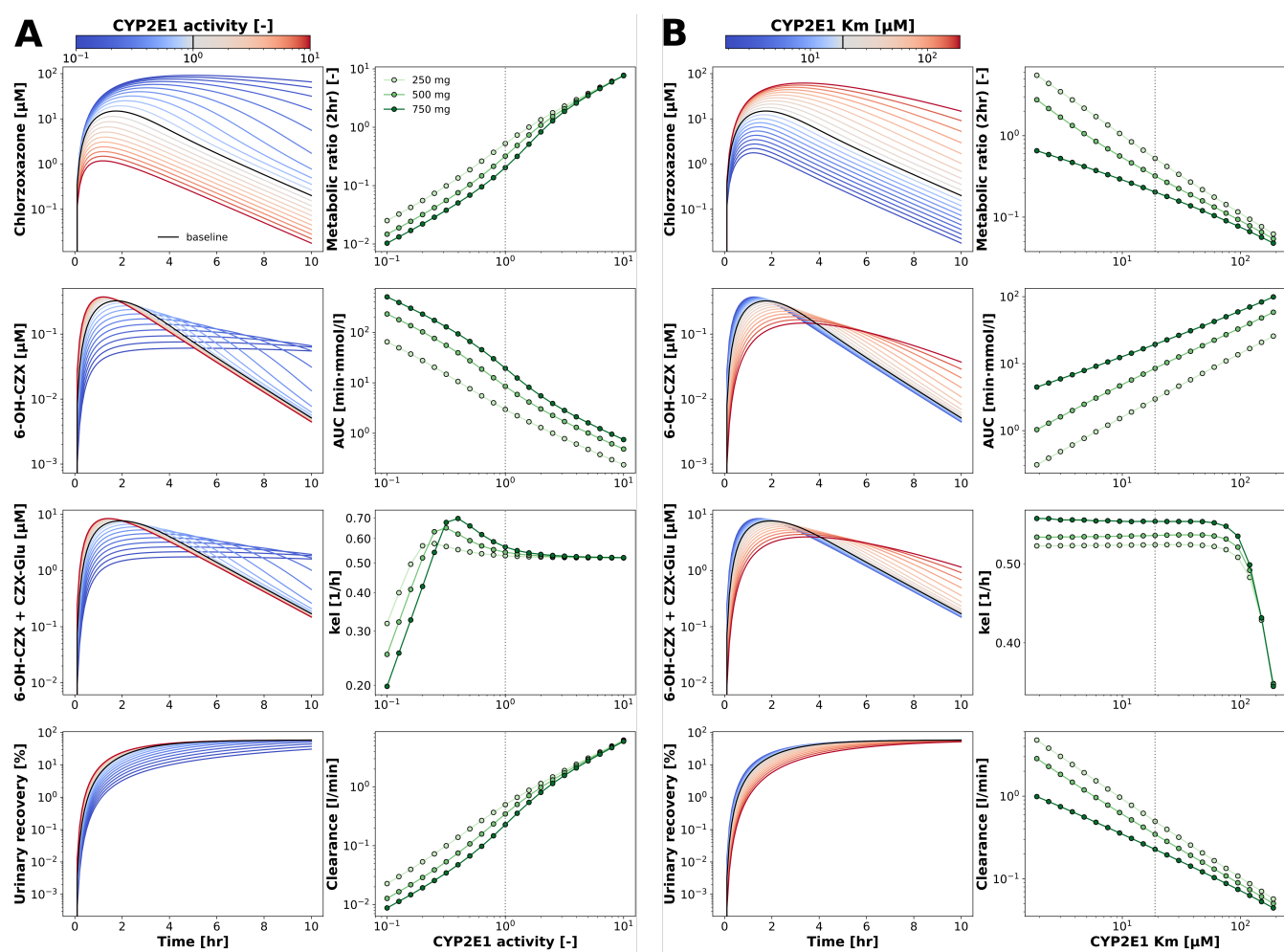


Figure 4: Parameter scans (A, B) Scan for the CYP2E1 activity and the K_M value, respectively. The parameters were scanned using a log range from (-1, 1) which was multiplied with the fitted reference value of the scanned parameter (CYP2E1 activity, 1; CYP2E1 K_M , 18.929 μM). The scan was repeated for three doses (250, 500, 750 mg), and the pharmacokinetic parameters metabolic ratios (2 hr), area under the curve (AUC), elimination rate (kel), and clearance were calculated. The time-courses for the 250 mg dose are shown on the left column, and the pharmacokinetic parameters in the right column.

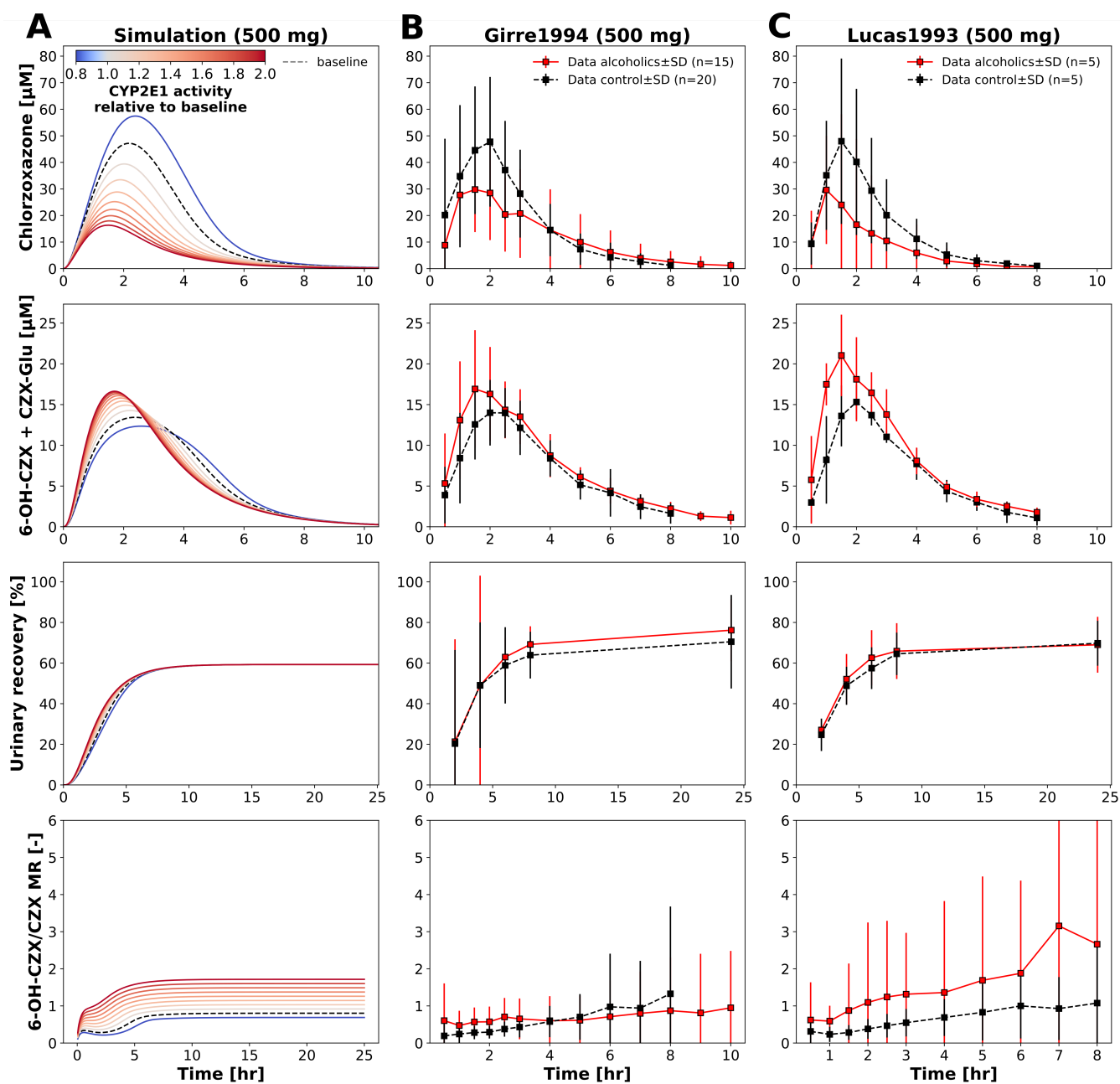


Figure 5: CYP2E1 induction in alcoholic subjects. (A) Parameter scan of the CYP2E1 activity. Simulated time-courses are shown, for plasma chlorzoxazone, chlorzoxazone-O-glucuronide, urinary recovery and metabolic ratio (2 hr). The black dashed line denotes the time-course belonging to the fitted baseline activity. (B, C) Time course data from (Girre et al., 1994; Lucas et al., 1993) for non-drinking control (black dashed line) and alcoholic subjects (red solid line). The metabolic ratios were calculated from the time-course data of chlorzoxazone and chlorzoxazone-O-glucuronide. The alcoholic subjects form (Girre et al., 1994) consumed (333 ± 191) g (mean \pm SD) of alcohol over (15.7 ± 10.7) h. No data about alcohol amounts consumed were reported by (Lucas et al., 1993). Both studies administered 500 mg of chlorzoxazone.

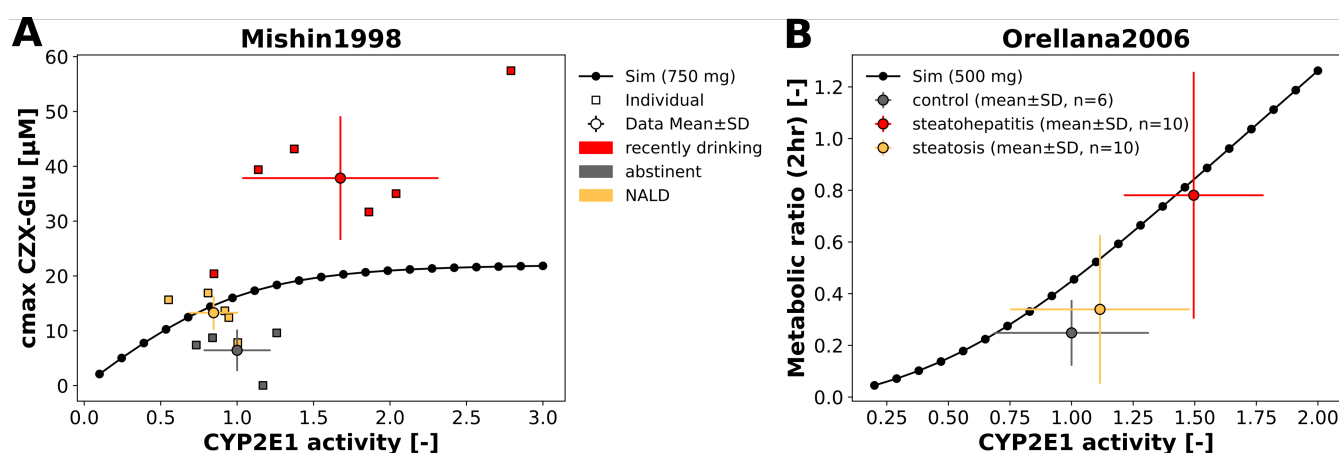


Figure 6: Predicted pharmacokinetics based in microsomal CYP2E1 concentrations. (A) Model prediction of the maximum concentration of plasma chlorzoxazone-O-glucuronide compared to data of (Mishin et al., 1998). (B) Model prediction of the metabolic ratio (2 hr) compared to data from (Orellana et al., 2006). The CYP2E1 activity parameter was scanned and the respective pharmacokinetic parameter was calculated. The microsomal protein concentrations reported by the studies were normalized so that the value of the abstinent (Mishin et al., 1998) or control group (Orellana et al., 2006) match the CYP2E1 activity of ($\text{LI_f_cyp2e1} = 1$).

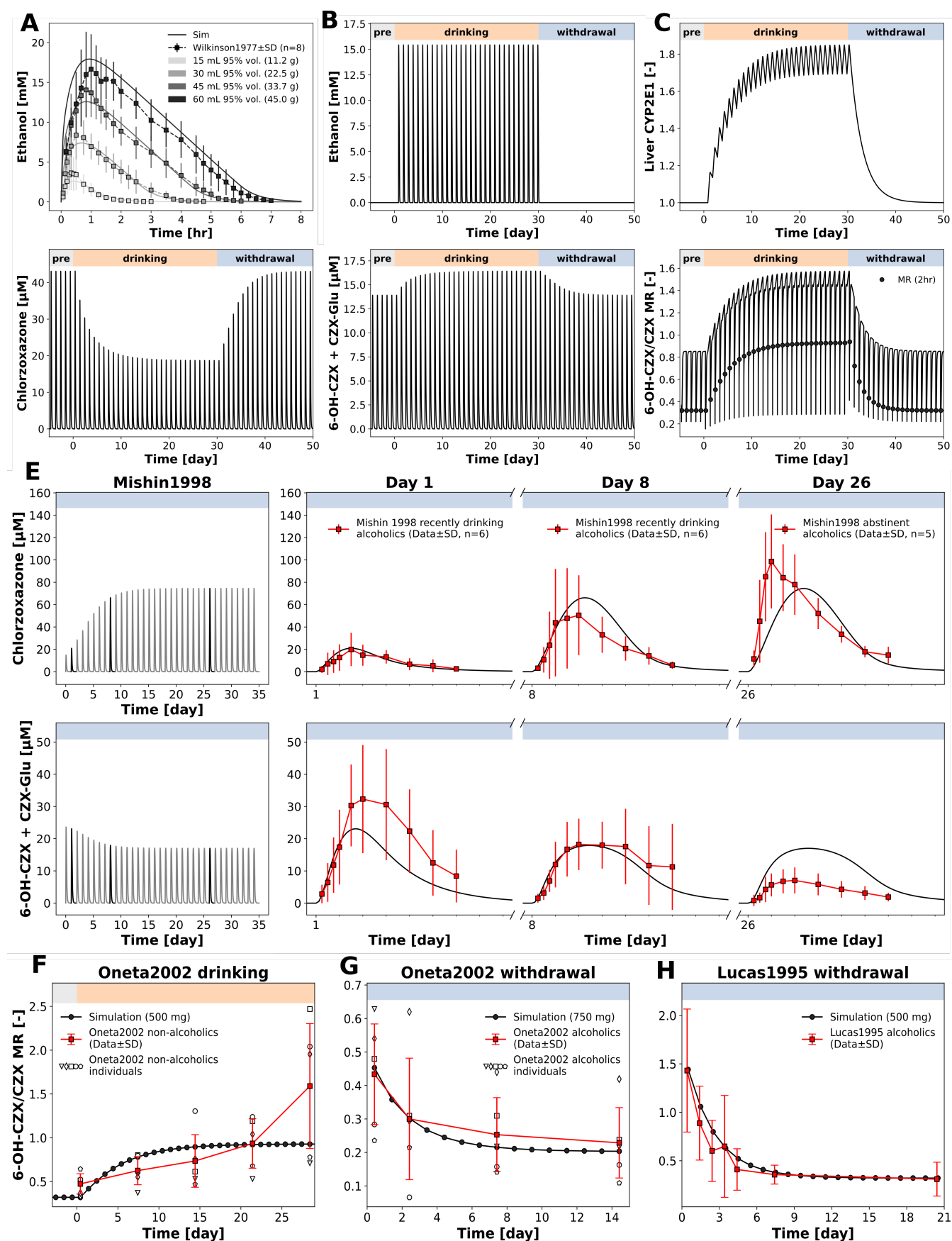


Figure 7: Effect of chronic ethanol consumption on the induction of CYP2E1 and chlorzoxazone pharmacokinetics We coupled the alcohol metabolism model with the chlorzoxazone pharmacokinetic model to study co administration of alcohol and chlorzoxazone over a time of multiple weeks. **(A)** The alcohol metabolism model was parametrized using data from (Wilkinson et al., 1977). The simulation experiment consists of three phases, The pre-drinking, drinking and withdrawal phase. Over all three phases a single chlorzoxazone dose was administered at 8:00 am. During the drinking phase, a single oral dose of 40 g alcohol was administered at 8pm **(B)**. The administration of alcohol causes an increase of the CYP2E1 level over time **(D)** and thereby affects the chlorzoxazone pharmacokinetics **(D)**. Several clinical studies investigated the change in chlorzoxazone pharmacokinetics during the start of drinking (Oneta et al. (2002)) and withdrawal (Mishin et al. (1998); Lucas et al. (1995); Oneta et al. (2002)). We used the model to simulate those studies in silico. For the simulation of the withdrawal studies Mishin1998 **(E)**, Oneta2002 **(G)**, and Lucas1995 **(H)**, the model was initialized with an initial CYP2E1 amount (LI_cyp2e1), such that the simulated time point (or time-course for chlorzoxazone for (Mishin et al., 1998)) at day 1 matched the corresponding data point. The initial CYP2E1 activity values were 3.0, 2.7 and 1.575 for Mishin1998, Lucas1995, and Oneta2002, respectively. The CYP2E1 half-life (LI_cyp2e1_thalf) was determined to be 1.8 d. For the simulation of the drinking group (Oneta et al. (2002)) the protocol, described above, was used. The inhibition constant ($LI_Ki_cyp2e1_deg_ethanol$) that determines how strongly alcohol inhibits the degradation of CYP2E1 was set to 0.01 μ M.

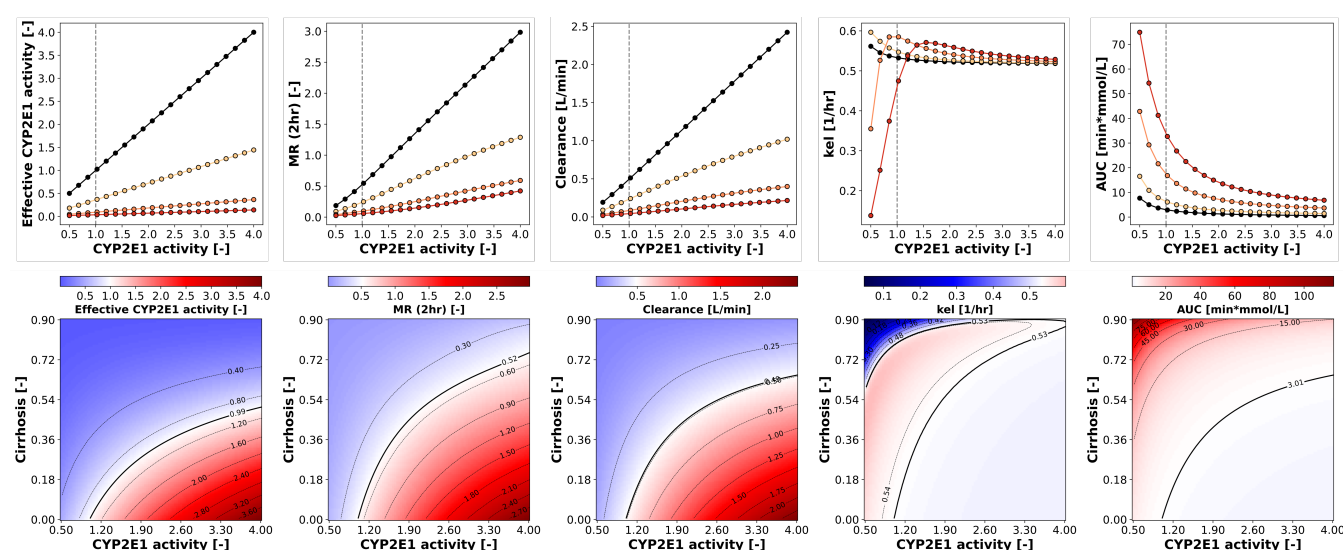


Figure 8: Combined effect of CYP2E1 induction and Cirrhosis. **(A)** Effect of the CYP2E1 activity on pharmacokinetic parameters for 4 different cirrhosis grades. A parameter scan for CYP2E1 (LI_f_cyp2e1) activity was performed for four Cirrhosis grades: Control ($f_{\text{cirrhosis}} = 0$), mild Cirrhosis ($f_{\text{cirrhosis}} = 0.40$), moderate Cirrhosis ($f_{\text{cirrhosis}} = 0.70$), severe Cirrhosis ($f_{\text{cirrhosis}} = 0.81$). **(B)** Two-dimensional continuous parameter scan for CYP2E1 activity (LI_f_cyp2e1) and cirrhosis grade ($f_{\text{cirrhosis}}$). Both parameters were scanned over a continuous range and the pharmacokinetic parameters were calculated. The resulting array was plotted as a heat map. The black lines mark the isoclines. The solid line denotes the isocline for the baseline value, i.e. the pharmacokinetic parameter calculated at $\text{LI_f_cyp2e1} = 1$ and $f_{\text{cirrhosis}} = 0$.

TABLES

Table 1: Overview of curated clinical studies.

References	PK-DB	PMID	Dosing protocol	Health status	Data	Fit	Validation
Bedada and Neerati (2016)	PKDB00621	26680654	250 mg, oral, single dose, tablet	healthy	plasma time-course (CZX, 6-OH-CZX*)	✓ *	
Bedada and Boga (2017)	PKDB00622	27670974	250 mg, oral, single dose, tablet	healthy	plasma time-course (CZX, 6-OH-CZX*)	✓ *	
Bedada and Neerati (2018)	PKDB00623	28983678	250 mg, oral, single dose, tablet	healthy	plasma time-course (CZX, 6-OH-CZX*)	✓ *	
Benowitz et al. (2003)	PKDB00623	14586387	250 mg, oral, single dose, tablet	healthy	plasma time-course (CZX), urinary recovery	✓	
Chalasani et al. (2003)	PKDB00623	12601351	500 mg, oral, single dose, tablet	healthy	plasma time-course (CZX), urinary recovery	✓	
Burkart et al. (1998)	PKDB00624	9542473	250 mg, oral, single dose, tablet	healthy	plasma time-course (CZX, 6-OH-CZX), urinary recovery	✓	
de Vries et al. (1994)	PKDB00626	7849234	250 mg, oral, single dose, tablet	healthy	plasma time-course (CZX), urinary recovery	✓	
Dreisbach et al. (1995)	PKDB00627	12534643	500 mg, oral, single dose, tablet	healthy	plasma time-course (CZX, 6-OH-CZX), urine time-course (6-OH-CZX)	✓	
Ernstgard et al. (2004)	PKDB00699	15255802	250, 500, 750 mg, oral, multiple dose, tablet	healthy	metabolic ratios, urinary recovery		✓
Frye et al. (1998)	PKDB00629	9597564	250, 750 mg, oral, multiple dose, tablet	healthy	plasma time-course (CZX, 6-OH-CZX), urine time-course (6-OH-CZX)	✓	
Girre et al. (1994)	PKDB00631	7910460	500 mg, oral, single dose, tablet	healthy, alcoholics	plasma time-course (CZX, 6-OH-CZX), urine time-course (6-OH-CZX)	✓	✓
He et al. (2019)	PKDB00632	31363741	400 mg, oral, single dose, tablet	healthy	plasma time-course (CZX)	✓	
Hohmann et al. (2019)	PKDB00633	31222796	0.005, 0.01, 0.05, 0.5, 5, 50 mg as solution, 250, 500 mg as tablet, oral, multiple dose	healthy	plasma time-course (CZX, 6-OH-CZX*)	✓	
Hukkanen et al. (2010)	PKDB00698	20233178	250 mg, oral, single dose, tablet	healthy	urinary recovery		✓
Kharasch et al. (1993)	PKDB00623	8513656	750 mg, oral, single dose, tablet	healthy	plasma time-course (CZX), urinary recovery	✓	
de la Maza et al. (2000)	PKDB00634	10832901	750 mg, oral, single dose, tablet	healthy	plasma time-course (CZX)	✓	
Liangpunsakul et al. (2005)	PKDB00636	15841467	500 mg, single dose, tablet	healthy	plasma time-course (CZX)	✓	
Lucas et al. (1993)	PKDB00637	8120116	500 mg oral, single dose, tablet	healthy, alcoholics	plasma time-course (CZX, 6-OH-CZX), urine time course (6-OH-CZX)	✓	✓
Lucas et al. (1995)	PKDB00688	7625570	500 mg oral, single dose, tablet	alcoholics	metabolic ratios		✓
Mishin et al. (1998)	PKDB00638	9820389	750 mg, oral, single dose, tablet	alcoholics	plasma time-course (CZX, 6-OH-CZX)	✓	
Oneta et al. (2002)	PKDB00689	7955797	500 mg, 250 mg, oral, multiple dose, tablet	alcoholics	metabolic ratios		✓
Orellana et al. (2006)		16321567	500 mg, oral, single dose, tablet	healthy, steatosis, steatohepatitis	metabolic ratios		✓
O'Shea et al. (1994)	PKDB00697	11804663	250 mg, oral, single dose, tablet	healthy	plasma time-course (CZX, 6-OH-CZX), urinary recovery	✓	
Park et al. (2006)	PKDB00641	16397290	400 mg, oral, single dose, tablet	healthy	plasma time-course (CZX, 6-OH-CZX)	✓	
Rajnarayana et al. (2008)	PKDB00643	19326774	250 mg, oral, single dose, tablet	healthy	plasma time-course (CZX)	✓	
Vesell et al. (1995)	PKDB00644	7773304	250 mg, oral, single dose, tablet	healthy	plasma time-course (CZX), urine time-course (6-OH-CZX)	✓	
Wang et al. (2003)	PKDB00639	12534643	500 mg, oral, single dose, tablet	healthy	plasma time-course (CZX), urinary recovery	✓	
Witt et al. (2016)	PKDB00640	27300008	5, 2.5, 0.5, 0.25, 0.05, 0.025, 0.005, 0.0025mg, oral, single dose, solution	healthy	plasma time-course (CZX, 6-OH-CZX*)	✓	
Wilkinson et al. (1977)	PKDB00700	881642	ethanol: 11.2, 22.5, 33.7, 45.0 g, oral, single dose, solution	healthy	plasma time-course (ethanol)		✓

* 6-OH-CZX was measured without the chlorzoxazone-O-glucuronide.

Table 2: Overview of model parameters.

Physiological parameter	Description	Value	Unit	Reference
BW	body weight	75	kg	ICRP (2002)
HEIGHT	body height	170	cm	ICRP (2002)
COBW	cardiac output per body weight	1.548	ml/s/kg	ICRP (2002); de Simone et al. (1997)
HCT	hematocrit	0.51		Vander (2001); Herman (2016)
f_lumen	fraction lumen of intestine	0.9		
FVgu	gut fractional tissue volume	0.0171	l/kg	Jones and Rowland-Yeo (2013); ICRP (2002)
FVli	liver fractional tissue volume	0.0021	l/kg	Jones and Rowland-Yeo (2013); ICRP (2002)
FVlu	lung fractional tissue volume	0.076	l/kg	Jones and Rowland-Yeo (2013); ICRP (2002)
FVve	venous fractional tissue volume	0.0514	l/kg	Jones and Rowland-Yeo (2013); ICRP (2002)
FVar	arterial fractional tissue volume	0.0257	l/kg	Jones and Rowland-Yeo (2013); ICRP (2002)
FVpo	portal fractional tissue volume	0.001	l/kg	Jones and Rowland-Yeo (2013); ICRP (2002)
FVhv	hepatic venous fractional tissue volume	0.001	l/kg	
FVgu	gut fractional tissue blood flow	0.018	l/kg	Jones and Rowland-Yeo (2013)
FQki	kidney fractional tissue blood flow	0.19		Jones and Rowland-Yeo (2013)
FQh	hepatic fractional tissue blood flow	0.215		Jones and Rowland-Yeo (2013)
Mr_czx	molecular weight CZX	169.56	g/mole	pubchem.compound/2733
Mr_czx6oh	molecular weight 6-OH-CZX	185.56	g/mole	pubchem.compound/2734
Mr_czxoglu	molecular weight CZX-O-Glu	361.69	g/mole	pubchem.compound/129522086
Mr_eth	molecular weight ethanol	46.07	g/mole	pubchem.compound/702
LI_Ki_cyp2e1_deg_ethanol	Ethanol-CYP2E1 inhibition constant	0.01	µM	adjustment by eye
LI_cyp2e1_thalf	half-time of CYP2E1	1.8	day	adjustment by eye
Fit parameter	Description	Value	Unit	
Ka_dis_tablet_czx	dissolution rate of chlorzoxazone tablet	0.521	1/hr	
GU_Ka_abs_czx	rate of gut chlorzoxazone absorption	1.325	1/hr	
GU_F_abs_czx	bio-availability for chlorzoxazone absorption	0.593	dimensionless	
LI_CZOX_Vmax	v _{max} for chlorzoxazone 6-hydroxylation	7.527	µmol/min/l	
LI_CZOX_Km	K _M value for 6-hydroxylation of chlorzoxazone	18.929	µM	
LI_CZXOGLU_Vmax	v _{max} for glucuronidation of 6-OH-CZX	11.346	µmole/min/l	
LI_CZXOGLU_Km	K _M for glucuronidation of 6-OH-CZX	0.255	µM	
KI_CZXOGLU_EX_k	urinary excretion rate of CZX-O-Glu	2.611	1/min	
GU_Ka_abs_eth	absorption rate of ethanol	2.59	1/hr	
LI_ETHEL_Vmax	v _{max} for ethanol elimination	0.033	mmole/min/kg	
LI_ETHEL_KM	K _M for ethanol elimination	0.046	mM	
Kp_ethanol	ethanol tissue partition coefficient	0.59	dimensionless	
Scan parameter	Description	Value	Unit	Range
LI_f_cyp2e1	scaling factor of CYP2E1 vactivity	1	dimensionless	0.1 - 100
LI_CZOX_Km	CYP2E1 K _M value	18.929	µM	1.8929 - 189.29